

Role of Podocyte B7-1 in Diabetic Nephropathy

Paolo Fiorina,^{*†} Andrea Vergani,^{*†} Roberto Bassi,^{*†‡} Monika A. Niewczas,[§] Mehmet M. Altintas,^{||} Marcus G. Pezzolesi,[§] Francesca D'Addio,^{*†} Melissa Chin,^{*} Sara Tezza,^{*} Moufida Ben Nasr,^{*} Deborah Mattinzoli,[¶] Masami Ikehata,[¶] Domenico Corradi,^{**} Valerie Schumacher,^{*} Lisa Buvall,^{††} Chih-Chuan Yu,^{††§§} Jer-Ming Chang,^{§§} Stefano La Rosa,^{|||} Giovanna Finzi,^{|||} Anna Solini,^{¶¶} Flavio Vincenti,^{***} Maria Pia Rastaldi,[¶] Jochen Reiser,[¶] Andrzej S. Krolewski,[§] Peter H. Mundel,^{††} and Mohamed H. Sayegh^{†††††}

^{*}Nephrology Division, Boston Children's Hospital, Harvard Medical School, Boston, Massachusetts; [†]Department of Medicine, San Raffaele Scientific Institute, Milan, Italy; [‡]DiSTeBA, Università del Salento, Lecce, Italy; [§]Section on Genetics and Epidemiology, Research Division, Joslin Diabetes Center and Department of Medicine, Harvard Medical School, Boston, Massachusetts; ^{||}Department of Medicine, Rush University Medical Center, Chicago, Illinois; [¶]Renal Research Laboratory, Fondazione IRCCS Ospedale Maggiore Policlinico and Fondazione D'Amico per la Ricerca sulle Malattie Renali, Milan, Italy; ^{**}Department of Biomedical, Biotechnological and Translational Sciences, Unit of Pathology, University of Parma, Parma, Italy; ^{††}Nephrology Division, Massachusetts General Hospital, Boston, Massachusetts; ^{†††}Graduate Institute of Medicine, College of Medicine, Kaohsiung Medical University, Kaohsiung, Taiwan; ^{§§}Department of Internal Medicine, Kaohsiung Medical University, Kaohsiung, Taiwan; ^{|||}Pathology Department, Ospedale di Circolo, Varese, Italy; ^{¶¶}Department of Clinical and Experimental Medicine, University of Pisa, Pisa, Italy; ^{***}Kidney Transplant Service, University of San Francisco, San Francisco, California; ^{††††}Transplantation Research Center, Brigham and Women's Hospital, Boston, Massachusetts; and ^{†††††}American University of Beirut, Beirut, Lebanon

ABSTRACT

Podocyte injury and resulting albuminuria are hallmarks of diabetic nephropathy, but targeted therapies to halt or prevent these complications are currently not available. Here, we show that the immune-related molecule B7-1/CD80 is a critical mediator of podocyte injury in type 2 diabetic nephropathy. We report the induction of podocyte B7-1 in kidney biopsy specimens from patients with type 2 diabetes. Genetic and epidemiologic studies revealed the association of two single nucleotide polymorphisms at the *B7-1* gene with diabetic nephropathy. Furthermore, increased levels of the soluble isoform of the B7-1 ligand CD28 correlated with the progression to ESRD in individuals with type 2 diabetes. *In vitro*, high glucose conditions prompted the phosphatidylinositol 3 kinase–dependent upregulation of B7-1 in podocytes, and the ectopic expression of B7-1 in podocytes increased apoptosis and induced disruption of the cytoskeleton that were reversed by the B7-1 inhibitor CTLA4-Ig. Podocyte expression of B7-1 was also induced *in vivo* in two murine models of diabetic nephropathy, and treatment with CTLA4-Ig prevented increased urinary albumin excretion and improved kidney pathology in these animals. Taken together, these results identify B7-1 inhibition as a potential therapeutic strategy for the prevention or treatment of diabetic nephropathy.

J Am Soc Nephrol 25: 1415–1429, 2014. doi: 10.1681/ASN.2013050518

Type 2 diabetes (T2D) is rapidly becoming the leading cause of ESRD.^{1,2} Despite much progress and an overall improvement in the treatment of diabetic nephropathy

(DN), the development of ESRD remains an epidemic problem.³ Podocyte foot processes, separated by narrow spaces, constitute the final barrier to urinary

Received May 21, 2013. Accepted November 19, 2013.

P.F., A.V., and R.B. contributed equally to this work.

Published online ahead of print. Publication date available at www.jasn.org.

Correspondence: Dr. Paolo Fiorina, Division of Nephrology, Boston Children's Hospital-Harvard Medical School, 300 Longwood Avenue, Enders Building, Fifth Floor, Room En511, Boston, MA 02115. Email: paolo.fiorina@childrens.harvard.edu

Copyright © 2014 by the American Society of Nephrology

protein loss by creating the porous membrane slit diaphragm, the integrity of which is essential for retaining proteins during filtration.^{4,5} A primary hallmark of DN is the progressive damage and death of glomerular podocytes,^{1,6–9} resulting in the leaking of proteins into the urine.⁴

B7-1 is an immune-related protein found on antigen-presenting cells that interacts with CD28 and CTLA4 on T cells, thus providing positive or negative costimulatory signals necessary for T-cell activation and survival.¹⁰ Induction of podocyte B7-1 is associated with development of proteinuria in human and murine lupus nephritis, in α_3 integrin knockout mice, in nephrin knockout mice, and in mice with LPS-induced proteinuria.⁵ The latter study also reported that podocytes exposed to LPS upregulate B7-1 *in vitro* and *in vivo*, thus leading to podocyte abnormalities and proteinuria.⁵ Of note, B7-1 knockout (B7-1^{-/-}) mice are protected from LPS-induced albuminuria, suggesting a causal link between podocyte B7-1 expression and proteinuria.⁵

Abatacept (CTLA4-Ig) is an inhibitor of B7-1 that is currently used to treat autoimmune diseases.¹¹ Here we show that high glucose induces podocyte B7-1 expression, thereby contributing to podocyte morphologic alterations and ultimately to DN, and that B7-1 blockade with CTLA4-Ig can protect podocytes from high glucose-induced injuries. These results suggest that the CD28/B7-1 pathway is relevant to the pathogenesis of T2D DN in humans, and CTLA4-Ig treatment may therefore offer a therapeutic strategy to combat DN. This notion is further supported by our recent findings showing that Abatacept is a therapy for proteinuria in patients with podocyte B7-1-positive FSGS.¹²

RESULTS

B7-1 Is Upregulated in Kidney Biopsies Obtained from a Subset of Patients with T2D and DN

To address whether B7-1 plays a role in human DN, we analyzed the expression of B7-1 in kidney biopsies of 30 individuals with T2D and DN at different stages of severity and from 30 controls (with surgically removed cancer-affected kidneys) (Figure 1). The demographic and metabolic characteristics of the individuals with T2D are displayed in Table 1. Among the samples, 14 biopsies (47%) from individuals with T2D and DN, but none of those obtained from controls, were positive for podocyte B7-1 expression (Figure 1, A, C, and D). Accordingly, real-time PCR on kidney biopsies showed increased B7-1 mRNA expression in individuals with T2D compared with controls (Figure 1B). To analyze B7-1 expression in our cohort of individuals with T2D, we divided our sample group based on a recently proposed DN pathologic classification.¹³ One individual with class 1 DN lesions showed high B7-1 expression (17% of the class 1 DN group) (Figure 1D), whereas individuals with class 2A–2B DN lesions showed moderate (25% of the class 2A–2B DN group) to high (25% of the class 2A–2B DN group) B7-1 expression (Figure 1D). Among individuals with T2D and DN class 3 renal pathologic evidence, 43% and 14% within this group showed moderate and high B7-1 expression, respectively (Figure 1D). Finally, the only patient with T2D classified as DN class 4 displayed high B7-1

expression (Figure 1D). Anecdotal cases of kidney biopsies with different degrees of glomerular B7-1 expression in individuals with T2D and various types of renal lesions are provided in Figure 1, E1–E5. Notably, high B7-1 expression levels parallel progressively reduced expression of synaptopodin, a cytoskeleton-associated podocyte-specific protein^{14,15} (Figure 1, F1–F5). This overlap with synaptopodin suggested podocyte localization of B7-1 (Figure 1, G1–G5; see Supplemental Table 1 for the list of antibodies used). B7-1 is thus upregulated in renal glomeruli from individuals with T2D and with different degrees of DN-related lesions.

Plasma Concentrations of sCD28 Determined at Baseline Are Associated with Future Risk of ESRD: Univariate and Multivariate Analyses

The soluble CD28 (B7-1 soluble ligand), a 44-kD protein, present in the peripheral bloodstream may be responsible for triggering podocyte B7-1. Interestingly, baseline plasma concentration of sCD28 was significantly higher in individuals who subsequently developed ESRD compared with individuals with preserved renal function (Supplemental Table 2). Nonparametric correlation coefficients of sCD28 with relevant baseline clinical characteristics were as follows: hemoglobin A1c (HbA1c), -0.02 ; albumin creatinine ratio (ACR), 0.25 ; and eGFR, -0.13 . We then examined the incidence rates of ESRD according to the quartiles of distribution of peripheral concentrations of sCD28 at baseline. Highest ESRD rates were observed among participants with high sCD28 concentrations, ESRD incidence rates were as follows: 1.7 for quartile 1 (Q1), 3.3 for Q2, 3.2 for Q3, and 6.0 for Q4 per 100 patient-years (P value for trend, $P=0.003$) (Figure 2A). When we examined the temporal pattern of ESRD occurrence according to baseline plasma concentrations of sCD28, the cumulative risk of ESRD for the highest quartile of sCD28 reached 66% within 12 years of follow-up, whereas it was 25%–38% for the remaining quartiles (P value for trend, $P=0.01$) (Figure 2B). None of the aforementioned results were evident across the quartiles of soluble B7-1 (sB7-1) distribution (data not shown). In a logistic regression model, the odds ratio (OR) of the subsequent progression to ESRD for individuals with high baseline concentrations of sCD28 (Q4) was 5.5 (95% confidence interval [95% CI], 2.0 to 14; $P=0.001$). In the multivariate analysis adjusted for clinical covariates at baseline, such as age, eGFR, HbA1c, and albuminuria (all of them as continuous variables), the independent ratio of odds of progression to ESRD among individuals with high concentrations of sCD28 (Q4) was 2.8 (95% CI, 1.0 to 7.8; $P=0.04$) (Figure 2C). The OR for sCD28 Q4, using a model with the same clinical covariates considered but including only patients followed for at least 5 years, was 4.8 (95% CI, 1.4 to 16; $P=0.01$). An increase in sCD28 peripheral levels may trigger podocyte B7-1, thus accelerating the decline in kidney function in individuals with T2D and DN.

B7-1 Is Upregulated in Podocytes in High Glucose Conditions *In Vitro*

Podocytes were cultured *in vitro* in the presence of normal glucose (NG) or high glucose (HG) for 7 and 14 days and

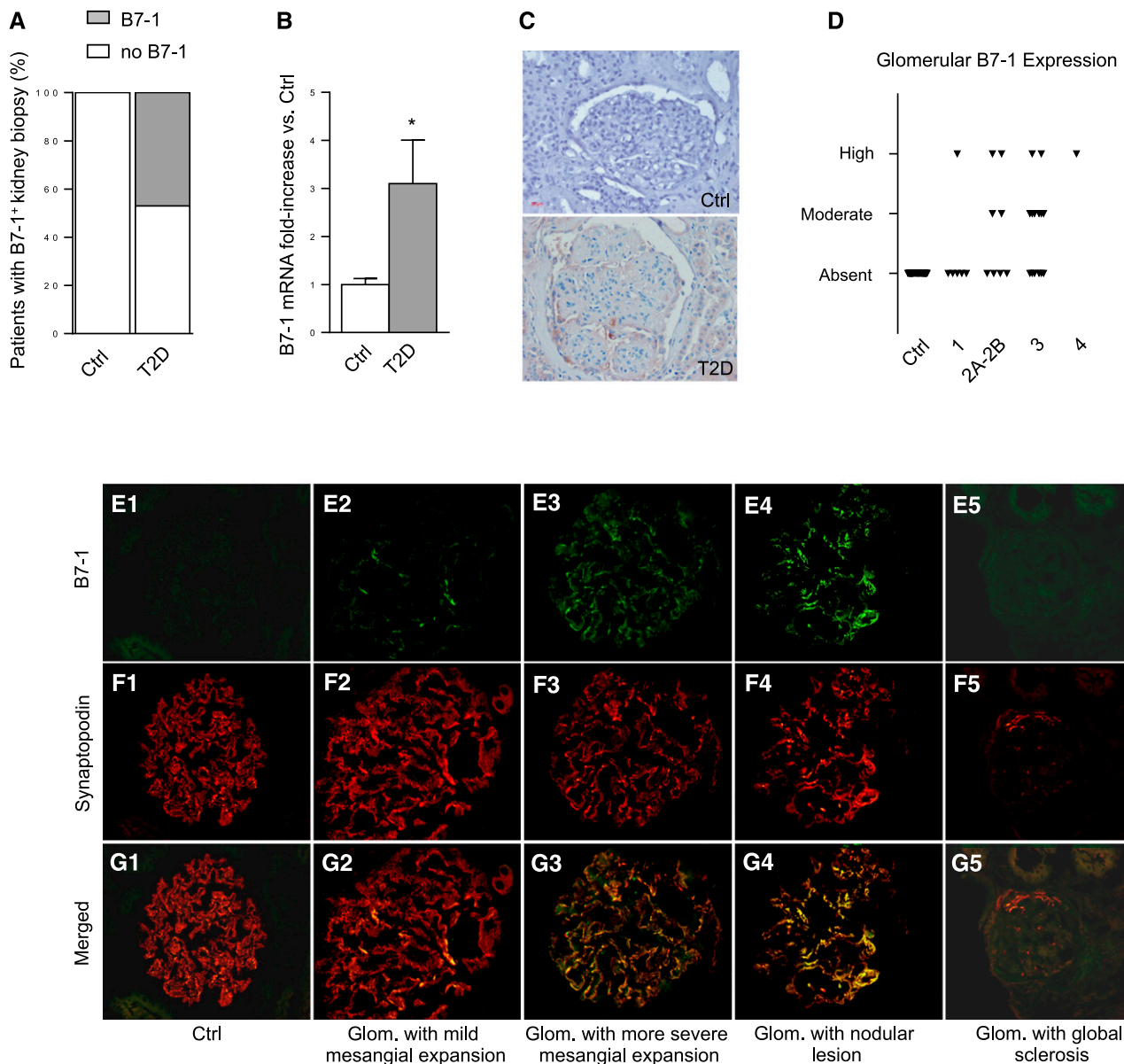


Figure 1. B7-1 is upregulated in kidney biopsies obtained from a subset of patients with T2D and DN-related lesions. Kidney biopsies obtained from individuals with T2D. (A, C, and D) B7-1 is expressed in 47% of biopsies obtained from individuals with T2D. (B) Real-time PCR analysis confirms an upregulation of B7-1 mRNA expression in individuals with T2D compared with controls ($*P < 0.05$). (D) Results show that 17% of individuals with T2D and belonging to DN class 1 have high B7-1 expression, whereas individuals with class 2A–2B DN lesions show moderate (25%) to high (25%) B7-1 expression. Among individuals with T2D and in DN class 3, 43% and 14% show a moderate and high B7-1 expression, respectively. Finally, the individual with T2D belonging to DN class 4 displays high B7-1 expression. (E1–E5) Anecdotal cases of kidney biopsies with different degrees of glomerular B7-1 expression in individuals with T2D and various types of renal lesions. (F1–F5) Notably, high B7-1 expression levels are paralleled by a progressively reduced expression of synaptopodin. (G1–G5) This overlap with synaptopodin suggests podocyte localization of B7-1. Ctrl, control; glom, glomerulus. Original magnification, $\times 200$.

B7-1 expression was evaluated by FACS analysis. Less than 2% of podocytes expressed B7-1 when cultured in NG for 14 days (Figure 3, A and H). Our results showed that 18% and 37% of podocytes were positive for B7-1 after 7 and 14 days of the HG condition, respectively, compared with NG and mannitol (serving as the osmotic control) (Figure 3, A and H). Notably, podocytes did not express other costimulatory molecules in

any of the conditions (Figure 3, B–G). Real-time PCR and Western blot analysis confirmed the increase of B7-1 mRNA and protein in podocytes cultured during HG conditions (Figure 3, I and J). B7-1 had perinuclear, cytoplasmic, and cellular process localization on immunofluorescence (Figure 3, L and M), which was absent in podocytes cultured in NG (Figure 3K) and mannitol (data not shown). Coexpression of B7-1 and

Table 1. Demographic and metabolic characteristics of individuals with type 2 diabetes who underwent kidney biopsy

| Patient | Age (yr) | Sex | DD (yr) | Creatinine (mg/dl) | UAE (mg/dl) | BUN (mg/dl) | GFR (ml/min) | HbA1c (%) | Cholesterol (mg/dl) | Triglycerides (mg/dl) | SBP (mmHg) | DBP (mmHg) | B7-1 (AU) |
|---------|----------|-------|---------|--------------------|-------------|-------------|--------------|-----------|---------------------|-----------------------|------------|------------|-----------|
| 1 | 61 | Man | 2 | 1.6 | 2.1 | 59 | 59 | 6.2 | 260 | 201 | 140 | 80 | 2 |
| 2 | 59 | Man | 3 | 1.3 | 1.0 | 66 | 40 | 5.4 | 213 | 99 | 140 | 80 | 0 |
| 3 | 44 | Man | 1 | 0.9 | 0.7 | 35 | 150 | 7.1 | 168 | 185 | 120 | 70 | 2 |
| 4 | 65 | Man | 17 | 2.1 | 4.3 | 68 | 38 | 6.3 | 231 | 114 | 140 | 90 | 0 |
| 5 | 63 | Man | 2 | 0.9 | 1.7 | 38 | 57 | 5.5 | 254 | 158 | 110 | 80 | 0 |
| 6 | 65 | Man | 12 | 0.7 | 3.4 | 25 | 114 | 8.9 | 267 | 195 | 150 | 80 | 1 |
| 7 | 77 | Woman | 4 | 0.7 | 2.3 | 36 | 120 | 5.2 | 160 | 100 | 160 | 90 | 2 |
| 8 | 48 | Man | 17 | 1.1 | 19.8 | 45 | 89 | 8.4 | 190 | 182 | 135 | 80 | 1 |
| 9 | 79 | Man | 4 | 2.4 | 1.6 | 67 | 40 | 5.9 | 250 | 180 | 140 | 60 | 0 |
| 10 | 54 | Man | 13 | 1.0 | 9.0 | 43 | 90 | 10.1 | 333 | 279 | 160 | 90 | 1 |
| 11 | 64 | Man | 5 | 1.2 | 0.6 | 41 | 108 | 8.0 | 151 | 188 | 150 | 80 | 1 |
| 12 | 65 | Woman | 10 | 1.1 | 4.8 | 78 | 54 | 7.6 | 230 | 484 | 140 | 80 | 0 |
| 13 | 64 | Man | 7 | 1.2 | 1.2 | 76 | 59 | 8.9 | 280 | 190 | 160 | 90 | 1 |
| 14 | 50 | Man | 3 | 1.1 | 2.0 | 38 | 100 | 8.1 | 241 | 314 | 150 | 90 | 2 |
| 15 | 59 | Man | 30 | 1.7 | 6.0 | 48 | 29 | 9.2 | 347 | 550 | 120 | 60 | 0 |
| 16 | 67 | Man | 20 | 1.5 | 6.0 | 39 | 98 | 8.2 | 195 | 263 | 140 | 70 | 1 |
| 17 | 56 | Man | 5 | 1.2 | 1.2 | 56 | 64 | 8.7 | 229 | 92 | 150 | 80 | 1 |
| 18 | 72 | Woman | 39 | 1.1 | 1.0 | 77 | 58 | 9.3 | 282 | 99 | 140 | 70 | 0 |
| 19 | 67 | Man | 14 | 1.2 | 2.0 | 41 | 58 | 6.4 | 224 | 138 | 145 | 90 | 0 |
| 20 | 58 | Man | 7 | 1.8 | 1.0 | 77 | 58 | 7.4 | 338 | 452 | 140 | 80 | 1 |
| 21 | 57 | Man | 7 | 1.1 | 2.9 | 34 | 84 | 7.9 | 161 | 302 | 150 | 90 | 2 |
| 22 | 46 | Man | 6 | 0.8 | 0.9 | 52 | 58 | 7.8 | 177 | 106 | 160 | 90 | 0 |
| 23 | 59 | Man | 20 | 1.1 | 1.9 | 45 | 49 | 7.5 | 151 | 85 | 150 | 90 | 0 |
| 24 | 40 | Man | 4 | 0.7 | 1.0 | 38 | 98 | 6.9 | 194 | 193 | 130 | 80 | 2 |
| 25 | 59 | Man | 3 | 0.9 | 0.4 | 41 | 102 | 8.3 | 200 | 150 | 120 | 80 | 0 |
| 26 | 59 | Man | 33 | 1.4 | 0.6 | 82 | 44 | 7.5 | 221 | 158 | 140 | 90 | 0 |
| 27 | 58 | Man | 4 | 1.2 | 0.8 | 50 | 98 | 7.6 | 155 | 109 | 140 | 90 | 0 |
| 28 | 61 | Man | 6 | 1.1 | 0.5 | 45 | 76 | 7.4 | 160 | 120 | 140 | 90 | 0 |
| 29 | 59 | Man | 6 | 1.2 | 0.6 | 43 | 90 | 7.2 | 140 | 98 | 130 | 80 | 0 |
| 30 | 62 | Woman | 32 | 1.8 | 4.0 | 65 | 17 | 8.0 | 350 | 480 | 130 | 70 | 0 |

DD, disease duration; SBP, systolic BP; DBP, diastolic BP; AU, arbitrary unit.

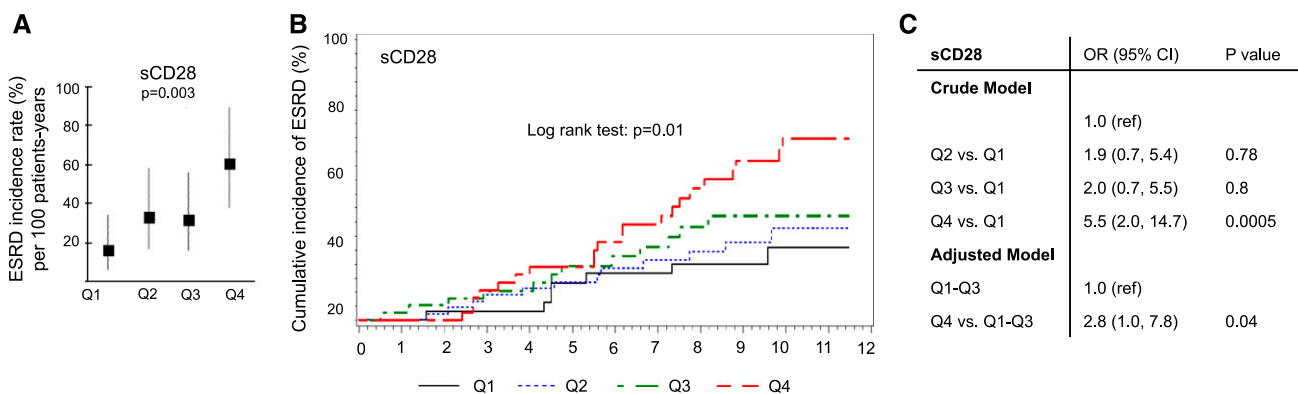


Figure 2. Elevated baseline plasma concentrations of sCD28 are associated with future risk of ESRD. (A) ESRD incidence rates are shown according to quartile distribution for the baseline plasma levels of soluble CD28 (sCD28). Low baseline sCD28 concentrations result in low ESRD incidence rates, whereas a progressive increase of marker concentration in the serum is associated with worse outcome. Incidence rates according to quartile distribution are as follows: Q1, 1.7; Q2, 3.3; Q3, 3.2; and Q4, 6.0 per 100 patient-years (** $P < 0.01$). (B) The cumulative risk for ESRD occurrence for Q4 of sCD28 reaches 66% within 12 years of follow-up, whereas it is 25%–38% for the remaining quartiles ($*P < 0.05$). (C) In a logistic regression model, the OR of the subsequent progression to ESRD for participants with high baseline concentrations of sCD28 (Q4) is 5.5 (95% CI, 2.0 to 14; $***P = 0.001$). Multivariate analysis adjusted for clinical covariates at baseline, such as age, eGFR, HbA1c, and albuminuria, shows an odds of progression ratio to ESRD of 2.8 (95% CI, 1.0 to 7.8; $*P = 0.04$) among patients with high concentrations of sCD28 (Q4).

synaptopodin suggested the podocyte origin of B7-1 (Figure 3, N–P). B7-1 is upregulated in podocytes in HG conditions.

B7-1 Upregulation Is Phosphatidylinositol 3-Kinase Dependent

The pathway that regulates B7-1 expression in podocytes in response to HG is largely unknown⁵; elucidation of this pathway may provide novel therapeutic targets and may confirm

the common pathway between HG and B7-1 upregulation. Three major intracytoplasmic key players appeared to be potentially related to both HG intracellular signaling and B7-1 expression: phosphatidylinositol 3-kinase (PI3K), serine/threonine protein kinase (AKT), and glycogen synthase kinase 3 (GSK3).^{16,17} AR-A014418 (0.2–2 μM) and triciribine (1–10 μM) (GSK3 and AKT inhibitors, respectively) did not affect B7-1 expression when added to podocytes cultured during HG

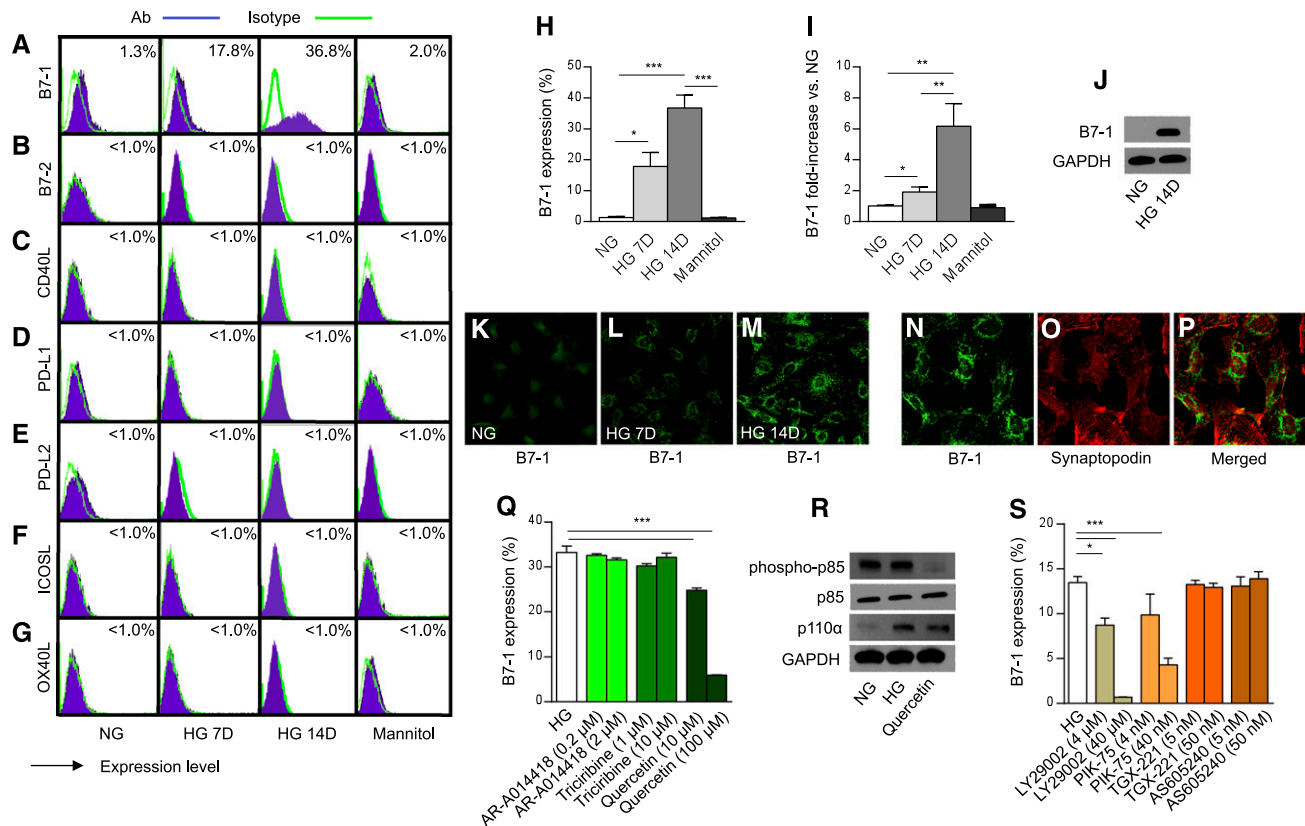


Figure 3. B7-1 is upregulated in podocytes in HG conditions *in vitro*. Conditionally immortalized podocytes are grown at 37°C in NG (10 mM) and HG (30 mM) for 7 and 14 days (D). Mannitol (20 mM plus glucose 10 mM) is used as an osmotic control. Cells are harvested, and the expression of multiple costimulatory molecules is evaluated by FACS analysis. B7-1 is barely expressed after 14 days of normal glucose or mannitol (A and H) culture conditions, whereas it increases after 7 and 14 days of HG conditions (* P <0.05; *** P <0.001, NG versus HG, 7D and HG14D, respectively; *** P <0.001, mannitol versus HG 14D). (B–G) All other costimulatory molecules tested are unchanged during HG. (I) Real-time PCR analysis confirms the increase of B7-1 mRNA after 7 and 14 days in high glucose compared with normal glucose (* P <0.05; ** P <0.01, NG versus HG 7D and HG 14D; ** P <0.01, HG 7D versus HG 14D). (J) Similarly, Western blot analysis shows greater B7-1 expression in podocytes cultured in HG after 14 days compared with those cultured in NG. (K–M) Immunofluorescence analysis confirms B7-1 expression in podocytes after 7 and 14 days of HG (L and M), but not after NG (K), conditions. (N–P) B7-1 is expressed on podocytes as shown by colocalization with synaptopodin, an actin-associated protein. To determine the pathway linking HG and B7-1 upregulation, we tested the effect of AKT, GSK3, and PI3K inhibitors on B7-1 expression. (Q) Although the AKT (triciribine) and GSK3 (AR-A014418) inhibitors are ineffective in downregulating B7-1 expression, the pan-PI3K inhibitor quercetin inhibits B7-1 upregulation (*** P <0.001, 10 and 100 μM quercetin versus HG). (R) Western blot analysis shows higher levels of phosphorylation of the p85 PI3K subunit and an increase in expression of the p110 α subunit upon HG culture, confirming the increased activity of the PI3K pathway after high glucose exposure. The PI3K inhibitor quercetin reduces both p85 phosphorylation and p110 α levels. (S) A more specific pan-PI3K inhibitor (LY29009) downregulates B7-1 expression as well (* P <0.01; *** P <0.001, HG versus LY29009 4 and 40 μM , respectively). Only the specific targeting of the p110 α PI3K subunit with PIK-75 (4–40 nM), but not of p110 β and p110 γ with TGX-221 (5–50 nM) and AS605240 (5–50 nM) respectively, was able to downregulate HG-dependent B7-1 expression in HG-cultured podocytes (*** P <0.001, HG versus PIK-75 4–40 nM). ab, antibody; PD-L1, programmed cell death ligand 1; PD-L2, programmed cell death ligand 2; ICOSL, inducible costimulator ligand; phospho, phosphorylated; GAPDH, glyceraldehyde-3-phosphate dehydrogenase.

for 14 days, despite demonstration of inhibition of GSK3 and AKT activity (Figure 3Q and data not shown). Conversely, quercetin (10–100 μM), a pan-PI3K inhibitor, was effective in reducing B7-1 expression in HG conditions (Figure 3Q). Western blot analysis revealed that in HG conditions, expression of the 110-kD catalytic PI3K α subunit (p110 α) was increased and phosphorylation of the regulatory subunit p85 was decreased compared with NG condition (Figure 3R and data not shown). A more specific PI3K inhibitor (LY29009), used for a shorter period of time and at different doses (4–40 μM) to avoid toxicity, was also effective in reducing B7-1 expression after 7 days of treatment (Figure 3S). We then confirmed the role of the p110 α subunit by using selective inhibitors of p110 α (PIK-75, 4–40 nM), p110 β (TGX-221, 5–50 nM), and p110 γ (AS605240, 5–50 nM) PI3K subunits. Only the p110 α -specific inhibitor was able to inhibit HG-dependent B7-1 upregulation (Figure 3S). HG-dependent B7-1 upregulation is mediated by the specific activation of the 110-kDa catalytic PI3K α subunit.

CTLA4-Ig Prevents HG-Induced Podocyte Cytoskeleton Disruption *In Vitro*

We examined the effect of CTLA4-Ig on HG-induced podocyte cytoskeleton abnormalities by immunofluorescence analysis. First, we were able to show that CTLA4-Ig, but not L6, binds to B7-1 on podocytes *in vitro* (Figure 4, A–D, Supplemental Material). Second, we observed that during CTLA4-Ig treatment, B7-1 appeared barely expressed upon immunofluorescence analysis in podocytes cultured in HG (Figure 4E4); however, B7-1 protein was detectable by Western blot, confirming that CTLA4-Ig was possibly masking B7-1 epitopes (Figure 4E4, inset). Furthermore, CTLA4-Ig, but not L6, prevented the HG-induced alteration of synaptopodin (Figure 4, E1–E4). Actin staining by phalloidin showed microfilament depolarization and signs of cytoskeleton derangement in HG, whereas CTLA4-Ig, but not L6, preserved actin and paxillin (a focal adhesion-associated protein activated after integrin-dependent cell adhesion¹⁸) original structures (Figure 4, F1–F4). $\alpha_3\beta_1$ integrin (a protein that physiologically participates in slit diaphragm formation and integrity¹⁹) activation is preserved by CTLA4-Ig but not L6 (Figure 4, G1–G4). Podocyte motility, assessed by an *in vitro* wound healing assay, was increased in podocytes exposed to HG conditions (Figure 4, I1, I2, and K) compared with podocytes cultured in NG (Figure 4, H1, H2, and K) and CTLA4-Ig therapy was able to prevent podocyte migration (Figure 4, J1, J2, and K). Finally, quantification of actin stress fibers further confirmed the derangement of the structure of the actin filaments in HG-cultured podocytes and the therapeutic effect of CTLA4-Ig (Figure 4, L1–L3 and M). Importantly, CTLA4-Ig prevented cytoskeleton and adhesion abnormalities in podocytes exposed to HG *in vitro*.

B7-1 Overexpression Induces Podocyte Morphologic Abnormalities

To clarify whether the overexpression of B7-1 or gene silencing of B7-1 expression in podocytes was able to mimic the effect of

HG and the protection mediated by CTLA4-Ig, we genetically upregulated and downregulated B7-1 expression. Podocytes were transduced with different lentiviral vectors carrying either the B7-1 cDNA sequence (VVWP–B7-1 or B7-1–overexpressing podocytes) or a specific small hairpin RNA (shRNA) sequence (pLKO.1–shRNA or B7-1 knockdown podocytes). B7-1 overexpression and downregulation were assessed by FACS and by Western blot analyses (Figure 5, A, B, E, and F). In NG and HG conditions (7 days), B7-1–overexpressing podocytes (>95% of B7-1⁺ podocytes; Figure 5A) showed a loss of synaptopodin staining in immunofluorescence analysis compared with wild-type (WT) podocytes. CTLA4-Ig therapy was able to prevent these alterations (Figure 5, C1–C3). Electron microscopy analysis showed an altered cellular morphology with dilated reticulum cisternae (Figure 5D2, red arrow) and numerous glycogen particles (Figure 5D2, white arrow) in the VVWP–B7-1 podocytes compared with WT (Figure 5, D1 and D2) and CTLA4-Ig–treated (Figure 5D3) podocytes. Conversely, pLKO.1 podocytes were similar to WT podocytes in terms of conserved synaptopodin expression (Figure 5, G1 and G2) and cellular ultrastructure (Figure 5, H1 and H2) when cultured in HG, whereas CTLA4-Ig did not exert any appreciable activity (Figure 5, G3 and H3). Transduction with VVWP–B7-1 and pLKO.1 control vectors did not modify podocyte morphology or ultrastructure compared with WT conditions (data not shown).

B7-1 Promotes Podocyte Cell Death

To better determine the role of the modulation of B7-1 expression on podocyte survival, we studied the effect of genetic overexpression and downregulation of B7-1 on podocyte apoptosis. B7-1–overexpressing podocytes cultured in NG (data not shown) and HG conditions for 7 days had higher apoptotic events compared with WT podocytes (Figure 5I), whereas podocytes in which B7-1 expression was downregulated had lower apoptosis rates compared with VVWP–B7-1 and similar apoptotic events to WT podocytes (Figure 5J). Finally, infection with VVWP–B7-1 and pLKO.1 control vectors, did not modify the percentage of apoptotic podocytes compared with WT cells (Figure 5, I and J).

B7-1 Induction Promotes Degradation of Synaptopodin and Loss of Stress Fibers

To explore a link between B7-1 expression and podocyte cytoskeleton disruption, we exposed podocytes to LPS, an established inducer of podocyte B7-1 expression.⁵ Induction of B7-1 expression caused degradation of synaptopodin (Figure 5K) and the loss of stress fibers in WT but not in B7-1 knockdown podocytes (Figure 5, L1–L3). Gene silencing of B7-1 preserved synaptopodin protein abundance and stress fiber integrity (Figure 5, K and L3).

Podocyte B7-1 Is Induced in Two Models of DN *In Vivo*

We evaluated podocyte B7-1 expression *in vivo* in two models of DN.²⁰ A progressive increase in B7-1 expression was

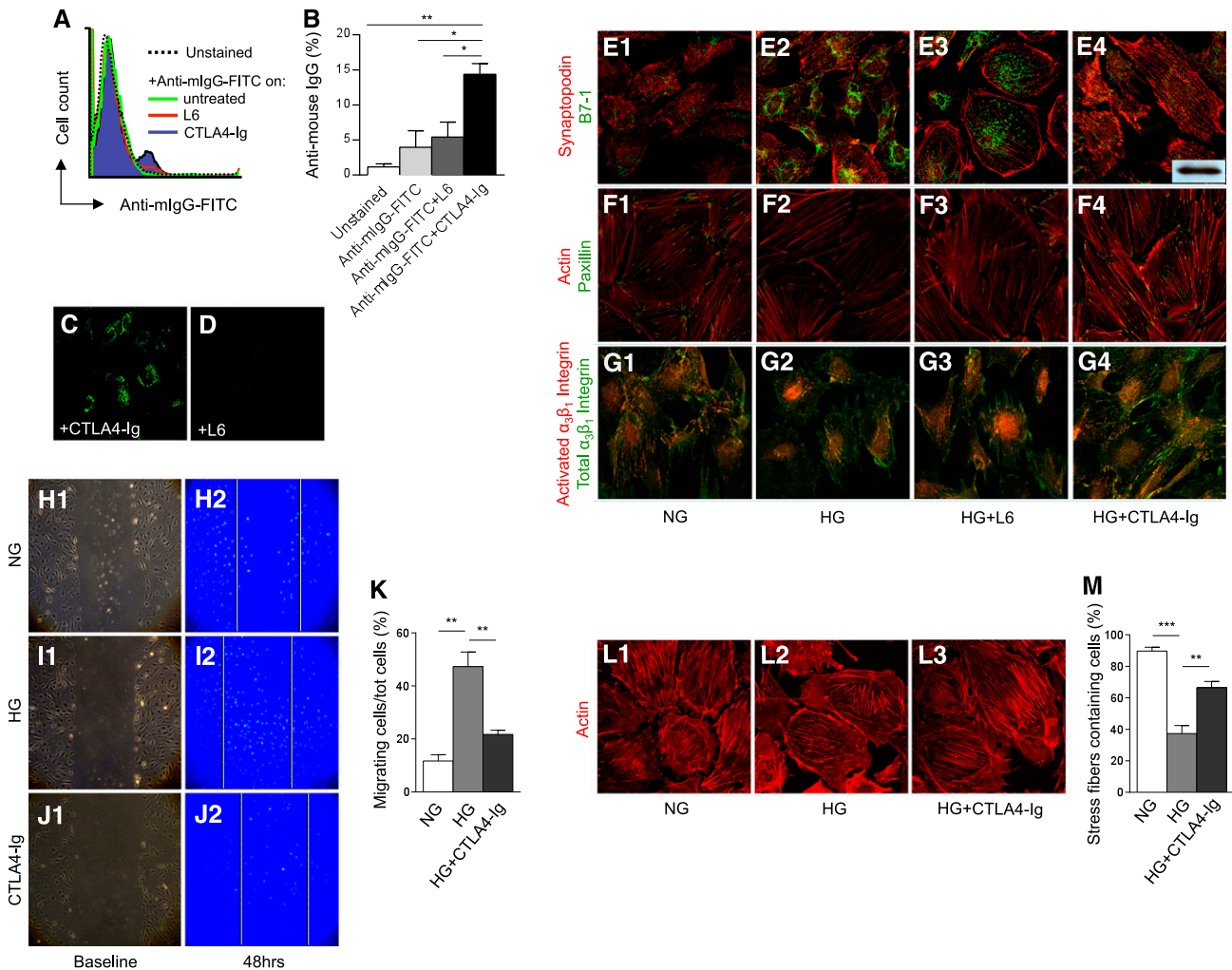


Figure 4. B7-1 activation leads to abnormalities of podocyte morphology and motility. (A and B) Podocytes cultured for 14 days in HG, untreated, or treated with CTLA4-Ig or L6 (100 $\mu\text{g}/\text{ml}$) are harvested and stained with FITC-conjugated anti-mouse IgG. Unstained, untreated, and L6-treated podocytes are not differentially stained by the FITC-conjugated anti-mouse IgG, but increased anti-murine-IgG-FITC staining is evident in podocytes treated with CTLA4-Ig (** $P < 0.01$; * $P < 0.05$, anti-murine-IgG-FITC+CTLA4-Ig versus unstained, anti-murine-IgG-FITC untreated and anti-murine-IgG-FITC+L6, respectively). (C and D) CTLA4-Ig binding, but not L6, is confirmed by indirect immunofluorescence with anti-murine-IgG-FITC. (E1–E4, F1–F4, G1–G4) Morphologic analysis of podocytes cultured in NG shows normal cytoskeleton organization (E1, F1, and G1); however, after HG exposure, severe actin depolymerization (red), synaptopodin (red), and paxillin (green) degradation as well as activated $\alpha_3\beta_1$ integrin (red) disruption are evident along with B7-1 upregulation (green) (E2, F2, and G2). CTLA4-Ig treatment (E4, F4, and G4), but not L6 (E3, F3, and G3), normalized most podocyte cytoskeleton abnormalities induced by HG. (H1, H2, I1, I2, and K) Podocytes exposed to HG for 48 hours display increased motility compared with podocytes cultured in NG (** $P < 0.01$, NG versus HG). (I1, I2, J1, J2, and K) CTLA4-Ig therapy prevented podocyte migration (** $P < 0.01$, HG versus CTLA4-Ig). (L1, L2, and M) HG-cultured podocytes show derangement of actin filaments compared with NG control podocytes (** $P < 0.001$, NG versus HG). (M) CTLA4-Ig is able to reinstate stress fiber integrity (** $P < 0.01$, HG versus CTLA4-Ig). Original magnification, $\times 400$.

observed in the glomeruli of leptin-deficient db/db mice with established DN compared with controls during follow-up (Figure 6, A1–A4 and B). Kidneys obtained from chemically-induced (*via* streptozotocin injection) hyperglycemic C57BL/6 mice were negative for B7-1 expression at 7 weeks of age (baseline) immediately after streptozotocin injection, whereas B7-1 expression was evident at 12 and 16 weeks of age (Figure 6, D1–D4 and E).

CTLA4-Ig Ameliorates Urinary Albumin Excretion in Diabetic Mice *In Vivo*

At 7 weeks of age, when hyperglycemia but not DN was present, db/db and streptozotocin-injected C57BL/6 were treated with CTLA4-Ig or L6 as follows: 500 μg induction regime at day 0; 250 μg at days 2, 4, 6, 8, and 10; and 250 μg twice a week until day 30. This dosage has been shown to inhibit B7-1 in a model of *in vivo* LPS-stimulated dendritic cell activation¹² as well as

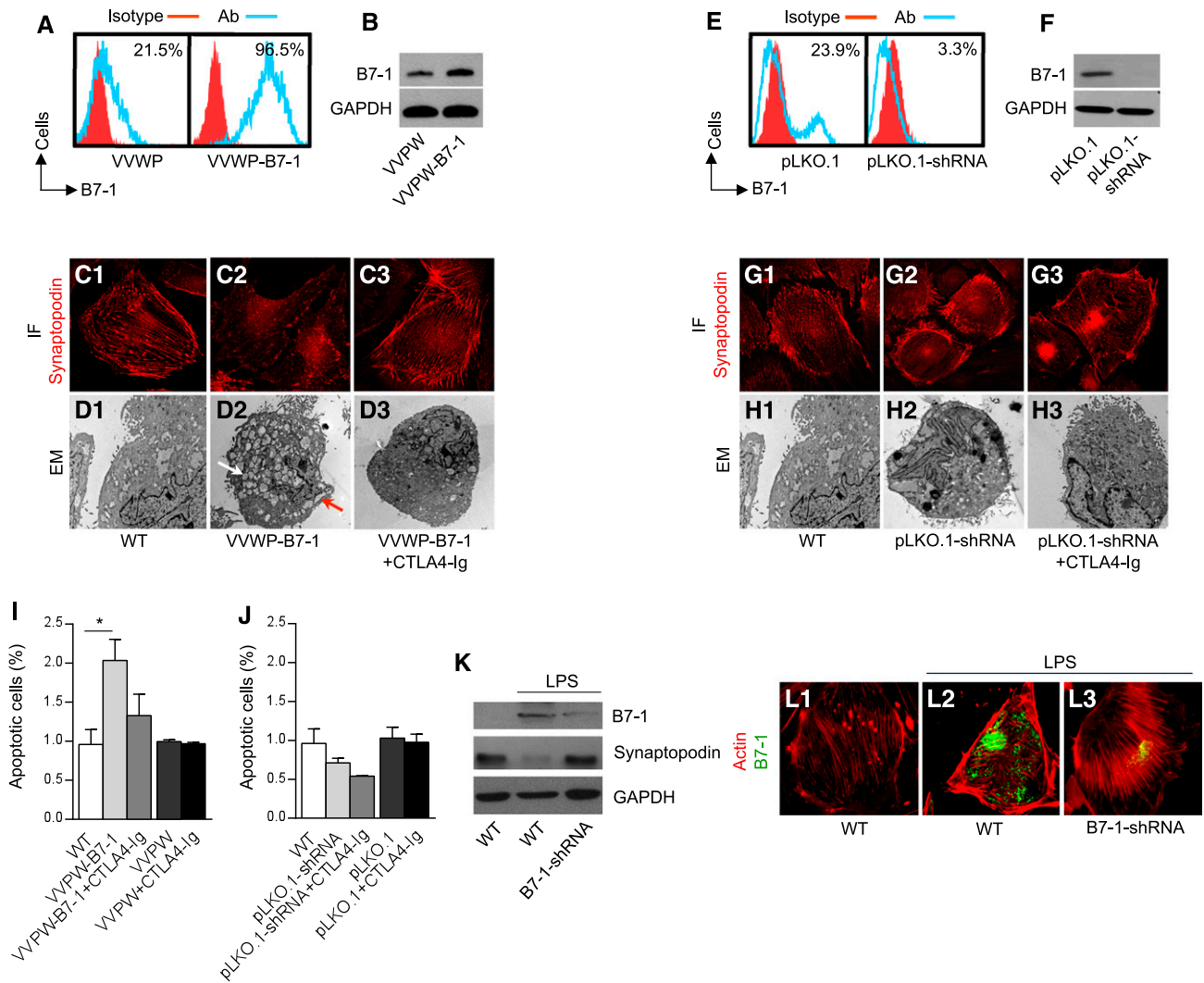


Figure 5. B7-1 genetic modulation impacts on podocyte morphology and survival. Podocytes are transduced with lentiviral vectors carrying either the B7-1 cDNA sequence (VVWP-B7-1 or B7-1-overexpressing podocytes) or a specific shRNA sequence (pLKO.1-shRNA or B7-1 knockdown podocytes). (A, B, E, and F) Successful transduction is assessed by FACS (A and E) and by Western blot analyses (B and F). (C1–C3 and D1–D3) Morphologically, VVWP-B7-1 podocytes showed a loss of synaptopodin staining (C2) with dilated reticulum cisternae (D2, red arrow) and glycogen particles (D2, white arrow) compared with WT (C1 and D1) and CTLA4-Ig-treated podocytes (C3 and D3). (G1–G3 and H1–H3) Downregulation of B7-1 using the pLKO.1-shRNA viral vector generates cell features comparable to WT podocytes with regard to synaptopodin degradation (G1–G3) and ultrastructural alterations (H1–H3). (I) VVWP-B7-1 podocytes display higher apoptotic events compared with WT podocytes ($*P < 0.05$, WT versus VVWP-B7-1). (J) pLKO.1-shRNA podocytes show levels of apoptosis comparable to WT podocytes. (I and J) Apoptosis is unmodified in podocytes transduced with control lentiviral vectors. (K) The LPS-induced degradation of synaptopodin is prevented in B7-1 knockdown podocytes. (L1) Double labeling for actin (red) and B7-1 (green) shows well developed stress fibers and absence of B7-1 in WT podocytes. (L2 and L3) The LPS-induced upregulation of B7-1 and the loss of stress fibers (L2) are prevented in B7-1 knockdown (B7-1-shRNA) podocytes (L3). ab, antibody; IF, immunofluorescence; EM, electron microscopy; GAPDH, glyceraldehyde-3-phosphate dehydrogenase.

in an *in vivo* model of chronic rejection.²¹ Although urinary albumin excretion increased in diabetic untreated db/db mice and L6-treated db/db mice (100 μ g/ml; Figure 6C), urinary albumin excretion remained stable over time in CTLA4-Ig-treated db/db mice (Figure 6C). In a second murine model of DN (streptozotocin-injected C57BL/6 mice), an increase in urinary albumin excretion was shown in diabetic untreated mice and L6-treated mice (Figure 6F) but not in CTLA4-Ig-

treated mice (Figure 6F). No increase in urinary albumin excretion was observed in nondiabetic control mice (Figure 6, C and F). We excluded the presence of any B7-1 tubular staining in db/db mice aged 7, 12, and 25 weeks (Figure 6, G1–G3) and demonstrated complete overlapping of B7-1 and the podocyte protein ZO-1 expression in db/db mice (Figure 6, H1–H3). Similarly, the percentage of mesangial expansion, another important feature of DN, increased in 25-week-old diabetic

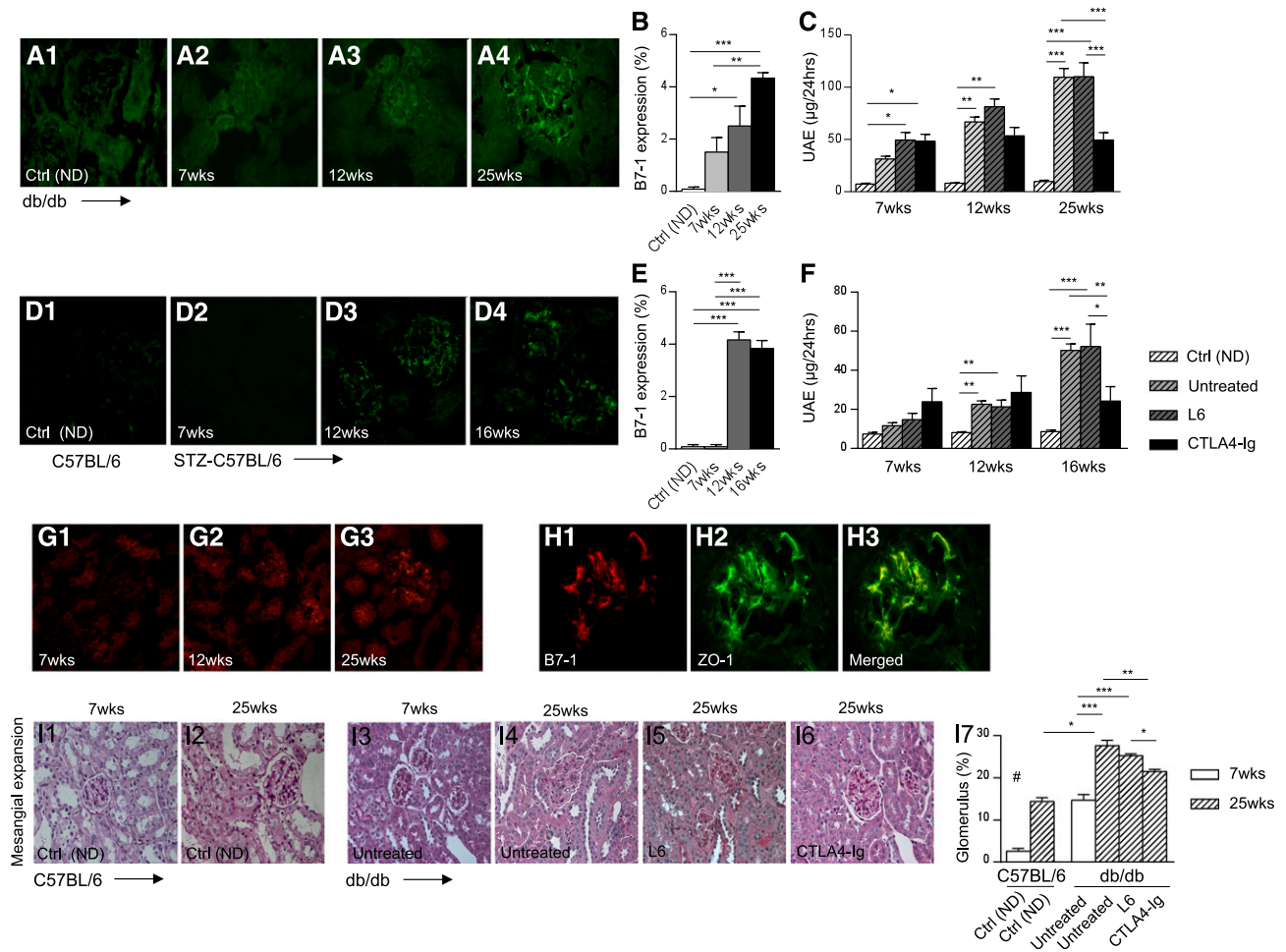


Figure 6. B7-1 immunofluorescence is performed in kidneys of two different murine models of DN. No B7-1 expression is observed in kidneys of control nondiabetic (Ctrl ND) heterozygous littermate db/db mice (A1 and B), whereas progressively increased B7-1 expression is noted in kidneys of 7-, 12- and 25-week-old db/db mice (A1–A4 and B) ($*P < 0.05$; $***P < 0.001$, control versus 12 and 25 weeks, respectively; $**P < 0.01$, 7 weeks versus 25 weeks). Db/db mice are randomly allocated to receive treatment with L6 ($n = 25$) or CTLA4-Ig ($n = 25$). (C) Significantly higher UAE levels are evident at 7, 12, and 25 weeks of age in db/db L6-treated mice and diabetic untreated db/db mice compared with controls ($*P < 0.05$, control versus L6-treated mice and CTLA4-Ig-treated mice at 7 weeks; $**P < 0.01$, control versus untreated and L6-treated mice at 12 weeks; $***P < 0.001$, control versus untreated and L6-treated mice at 25 weeks). On the contrary, UAE levels remain stable over time in CTLA4-Ig-treated mice ($***P < 0.001$, CTLA4-Ig versus untreated and L6-treated mice at 25 weeks). (D1, D2, and E) Absent B7-1 expression is observed in control C57BL/6 mice (7 weeks of age) (D1 and E) and in 7-week-old hyperglycemic C57BL/6 mice immediately after streptozotocin injection (D2 and E). (D3 and D4 and E) An increase in B7-1 expression is detected in 12- and 16-week-old hyperglycemic C57BL/6 mice after streptozotocin injection ($***P < 0.001$, control versus 12 and 16 weeks; $***P < 0.001$, 7 weeks versus 12 and 16 weeks). (F) Untreated diabetic C57BL/6 mice and L6-treated C57BL/6 mice show higher UAE at 12 and 16 weeks of age compared with control mice ($**P < 0.01$, control versus untreated and L6-treated mice at 12 weeks; $***P < 0.001$, control versus untreated and L6-treated mice at 16 weeks). Conversely, UAE levels remained stable over time in CTLA4-Ig-treated mice ($**P < 0.01$; $*P < 0.05$, CTLA4-Ig versus untreated and L6-treated mice at 16 weeks, respectively). Kidney parenchyma immunofluorescence showed absence of tubular B7-1 expression (G1–G3) and colocalization of B7-1 with ZO-1 (H1–H3) in db/db mice, demonstrating the podocyte localization of B7-1. Low levels of mesangial expansion are detectable in control nondiabetic C57BL/6 mice at 7 and 25 weeks of age ($^{\#}P < 0.05$, control versus all) (I1, I2, and I7) and in untreated db/db mice at 7 weeks of age (I3 and I7). (I3–I5 and I7) Conversely, increased mesangial expansion is evident at 25 weeks of age in untreated and L6-treated diabetic db/db mice compared with untreated db/db mice at 7 weeks of age ($***P < 0.001$, db/db: untreated [7 weeks] versus untreated [25 weeks] and L6-treated mice). (I4–I7) CTLA4-Ig-treated diabetic db/db mice have lower mesangial expansion compared with untreated and L6-treated diabetic db/db mice at 25 weeks of age ($**P < 0.01$; $*P < 0.05$, CTLA4-Ig-treated versus untreated [25 weeks] and L6-treated mice, respectively). Original magnification, $\times 1000$ in G1–G3 and H1–H3; $\times 250$ in I4–I7.

untreated mice and L6-treated mice compared with 25-week-old nondiabetic and CTLA4-Ig-treated mice (Figure 6, I1–I7). CTLA4-Ig also reduces collagen I deposition (Figure 7, A1–A4), preserves podocytes and nephrin/ZO-1 expression (Figure 7, B1–B4 and C1–C4, respectively), and reduces glomerular active caspase 3–positive (Figure 7, D1–D4) and terminal deoxynucleotidyl transferase–mediated digoxigenin–deoxyuridine nick-end labeling–positive nuclei (Figure 7, E1–E4) in db/db mice aged 25 weeks *in vivo* compared with L6-treated or untreated diabetic mice at the same time point. The aforementioned effects are obtained without affecting peripheral serum glucose (Figure 7F), creatinine (Figure 7G), and cytokine levels (Figure 7, H–J).

Two Single Nucleotide Polymorphisms of the B7-1 Gene Are Associated with the Progression of DN to ESRD

To confirm that the B7-1/CD28 axis is relevant for DN in humans, we used samples from the Joslin Study of Genetics of Nephropathy in individuals with T2D (Supplemental Figure 1, Supplemental Table 3). This cohort is composed of individuals with T2D monitored for 8–12 years of follow-up and censored for decline in renal function, onset of proteinuria, and ESRD. To evaluate whether any polymorphism in the *B7-1* gene could affect DN onset or progression, we screened and genotyped 173 individuals with T2D, DN, and either microalbuminuria ($n=3$), proteinuria ($n=138$), or ESRD ($n=32$) as well as 177 normoalbuminuric individuals. Genotypic associations with DN, ACR, and eGFR for single-nucleotide polymorphisms (SNPs) genotyped across the *B7-1* locus are shown in Supplemental Tables 3 and 4. The strongest association with the progression to ESRD, or with the worsening of ACR and decline in eGFR, in this population occurred at rs2629396 (OR, 1.56; $P=0.01$), a SNP located in intron 4 (position IVS4-183) of the *B7-1* gene (Supplemental Figure 1, A–C, Supplemental Table 3). A comprehensive analysis of imputed SNPs across this region identified a strong association at a second SNP (rs1523311) in complete linkage disequilibrium ($r^2=1.0$) with rs2629396 and located in intron 5 of *B7-1* (position IVS5+388) (Supplemental Table 4). Although these data highly suggest the relevance of B7-1 in the progression of DN to ESRD, these associations did not achieve statistical significance when a conservative Bonferroni correction was applied (threshold for significance: $0.05/12=0.00042$; corrected $P=0.01$). None of the SNPs evaluated at the *CD28* locus were shown to be associated with ESRD, ACR, or eGFR.

DISCUSSION

DN is a serious complication faced by individuals with T1 and T2D.^{1,2,22} Despite the extensive use of angiotensin-converting enzyme inhibitors and renin-angiotensin system blockers and the overall improvement in glycemic and BP control therapies, the burden of DN has not declined and DN remains a

primary cause of ESRD onset.^{23,24} Several of the recently tested approaches have failed to provide clear benefits,^{25–29} whereas others have offered such a narrow therapeutic window³⁰ that the pursuit for novel therapeutic approaches is necessary.

Our data show that B7-1 expression represents a common response of podocytes to HG and hyperglycemia, given that B7-1 is upregulated in podocytes *in vitro*, in hyperglycemic mice *in vivo*, and in individuals with T2D. Our results showed that 47% of individuals with T2D had B7-1 expression; however, the upregulation of podocyte B7-1 expression was evident in the early phase of DN, whereas B7-1 was mainly absent in individuals with T2D and diffused glomerulosclerosis. It is possible that B7-1 positivity defines a subgroup of individuals with T2D, proteinuria, and altered GFR, thus reconciling the dichotomy between proteinuria and decline in GFR that is found in some individuals with T2D and DN. Under the latter hypothesis, the presence of B7-1 may indeed define a group of individuals at higher risk for the progression of DN.

Genetic and epidemiologic analyses confirmed the relevance of B7-1 for DN. We identified two SNPs of the *B7-1* gene (rs2629396 and rs1523311), which appeared to be correlated with DN incidence, with the worsening of ACR and decline of eGFR over time. These two SNPs of the *B7-1* gene are located in two intron regions (4 and 5) of chromosome 3, which may constitute a DN-susceptible locus. Baseline plasma concentrations of soluble CD28 (the natural ligand of B7-1) were markedly increased in individuals who subsequently developed ESRD; indeed, it is possible, although unproven by our data, that soluble CD28 may trigger B7-1 activation on podocytes, thus leading to morphology abnormalities, including marked alteration of cytoskeleton structure. The genetic and epidemiologic analysis of the Joslin cohort of individuals with T2D establish the blueprint that the B7-1/sCD28 axis is relevant for the progression of DN. The upregulation of B7-1 expression in podocytes is specific and is not the result of a global increase of all costimulatory molecules due to inflammation, because B7-1 is the only costimulatory molecule upregulated on podocytes in HG conditions, possibly through a PI3K p110 α -dependent mechanism. B7-1 upregulation may *per se* induce podocyte cytoskeleton abnormalities, as suggested by our B7-1 genetic modulation studies.

Finally, according to our peripheral cytokine profiling and our *in vitro* podocyte studies, CTLA4-Ig action seems to take place independently of any anti-inflammatory or immunomodulatory effect, but, rather, through a podocyte-specific protective mechanism that ultimately prevents cellular abnormalities. Interestingly, drugs targeting B7-1 (CTLA4-Ig) are available for treating autoimmune diseases and in kidney transplantation (*e.g.*, abatacept and belatacept).¹¹ Multiple trials based on CTLA4-Ig are currently ongoing,^{31,32} with almost 2000 individuals already treated and an overall rate of side effects comparable to the placebo arm.^{11,33} We acknowledge that different limitations are present in our study. First, we did not demonstrate a major salutary effect of CTLA4-Ig on DN.

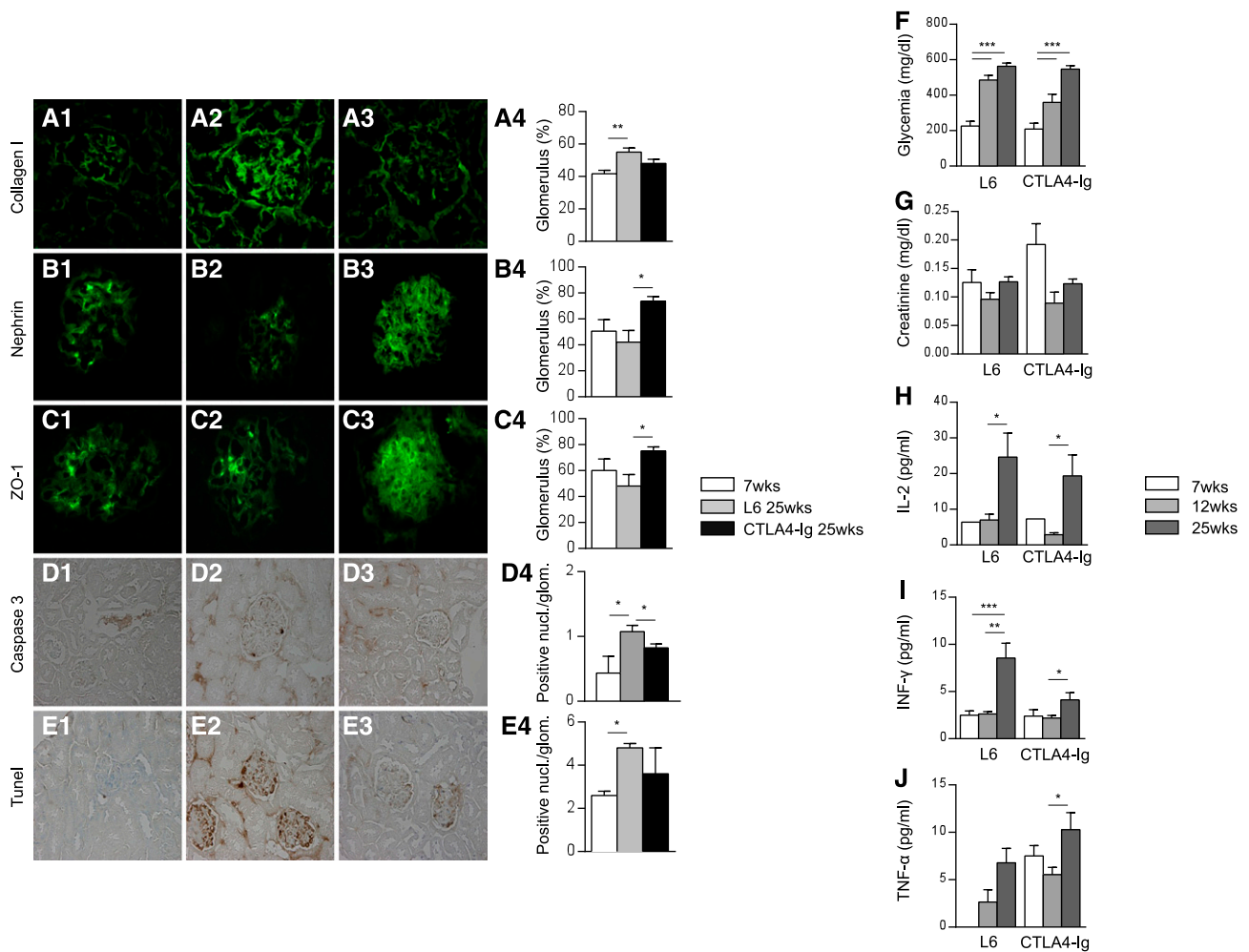


Figure 7. Morphologic and immunofluorescence analyses are performed on kidney samples obtained from untreated 7-week-old or from 25-week-old L6-treated mice or CTLA4-Ig-treated mice. Collagen I deposition is increased in L6-treated compared with CTLA4-Ig-treated and 7-week-old untreated db/db mice (** $P < 0.01$, L6-treated mice at 25 weeks versus 7 weeks) (A1–A4), nephrin (* $P < 0.05$, L6-treated mice at 25 weeks versus CTLA4-Ig-treated mice at 25 weeks) (B1–B4), and ZO-1 (* $P < 0.05$, L6-treated mice at 25 weeks versus CTLA4-Ig-treated mice at 25 weeks) (C1–C4) expression is preserved in CTLA4-Ig-treated mice compared with those treated with L6. (D1–D4) Increased expression of glomerular active caspase 3 is also evident in L6-treated mice compared with CTLA4-Ig-treated mice and 7-week-old untreated db/db mice (* $P < 0.05$, L6-treated mice at 25 weeks versus CTLA4-Ig-treated mice at 25 weeks and untreated mice at 7 weeks). (E1–E4) TUNEL staining shows higher levels of apoptosis in 25-week-old L6-treated mice compared with 7-week-old untreated mice (* $P < 0.05$, L6-treated mice at 25 weeks versus untreated mice at 7 weeks). (F and G) Serum glucose and creatinine levels are not different between 12 and 25 weeks of age between L6-treated mice and CTLA4-Ig-treated db/db mice ($P = NS$). (H–J) Peripheral levels of Th1 cytokines are increased over time in both L6-treated mice (* $P < 0.05$, IL-2: L6-treated mice at 25 weeks versus 12 weeks; *** $P < 0.001$; ** $P < 0.01$, IFN- γ : L6-treated mice at 25 weeks versus 12 and 7 weeks, respectively) and CTLA4-Ig-treated db/db mice (* $P < 0.05$, IL-2: CTLA4-Ig-treated mice at 25 weeks versus 12 weeks; * $P < 0.05$, IFN- γ : CTLA4-Ig-treated mice at 25 weeks versus 12 weeks; * $P < 0.05$, TNF- α : CTLA4-Ig-treated mice at 25 weeks versus 12 weeks). TUNEL, terminal deoxynucleotidyl transferase–mediated digoxigenin-deoxyuridine nick-end labeling; nucl, nuclei; glom, glomeruli. Original magnification, $\times 630$ in A1–A4, B1–B4, C1–C4; $\times 400$ D1–D4.

Second, the use of better models of diabetic glomerulopathy would have been potentially more meaningful. The lack of major differences noted in glomerular basal membrane thickness and in the number of WT1⁺ cells among groups (Supplemental Figure 3A) may be related to the less than severe DN that occurs in db/db mice. Unfortunately, the few remaining murine models of DN (e.g., OVE26 mice) may not be

appropriate for the study of B7-1 expression. Although the OVE26 mouse expresses a chicken calmodulin minigene controlled by the rat insulin II promoter and develops severe DN within weeks after birth,³⁴ we were not able to detect any B7-1 expression in the glomeruli of OVE26 mice. This absence of B7-1 expression could be due to the presence of a high-affinity binding site for calmodulin on PI3K,³⁵ so that manipulation of

calmodulin may interfere with PI3K activity and ultimately with B7-1 expression.³⁵

In conclusion, HG and hyperglycemia elicit B7-1 activation on podocytes, thereby potentially creating a therapeutic platform for the use of specific B7-1–targeting strategies for the treatment of proteinuria in DN (Figure 8) as shown by our recent findings showing the efficacy of Abatacept (CTLA4-Ig) in patients with podocyte B7-1–positive FSGS.¹²

CONCISE METHODS

Human Kidney Biopsies

Participants provided written informed consent and the Ospedale San Carlo (Milan, Italy) institutional review board approved this study. Kidney biopsies obtained from individuals with T2D ($n=30$) at different stages of DN were collected. For every individual, a record of medical history was available and serum and urine were collected to obtain kidney functional data. Histologic samples obtained from the unaffected kidney pole of individuals who underwent unilateral nephrectomy for renal cancer ($n=30$) served as controls. Table 1 provides demographic and metabolic details of our cohort.

Genetic Studies in the Joslin Clinic Cohort

Study Population and Genotyping

A detailed description of the Joslin Study of Genetics of Nephropathy in T2D collection was recently published.³⁶ We randomly selected 173 patients with DN with proteinuria, ESRD, or microalbuminuria and CKD stage 4 or 5, along with 177 normoalbuminuric controls from this collection, for whole genome genotyping on Illumina's Human CNV370v1 genotyping array (data available in dbGaP, <http://www.ncbi.nlm.nih.gov/gap/>, accession number phs000302.v1.p1) (Illumina, San Diego, CA). Previously described quality control measures were applied to these data.³⁷ The application of quality control metrics for minor allele frequency <0.01 , rejection of Hardy–Weinberg assumptions ($P \leq 10^{-5}$), and differential rates of missing data (by case/control status) resulted in high-quality genotypic data for 324,382 autosomal SNPs. The application of quality control criteria reduced the study population from 350 to 326 individuals of European ancestry. For case/control comparisons, strict phenotypic classification restricted our analysis to 142 patients with DN (113 proteinuric and 29 ESRD) and 151 normoalbuminuric controls. ACR and eGFR data from all 326 individuals of European ancestry were available for quantitative trait analysis. Genotypic data for all SNPs mapping to the *B7-1* and *CD28* loci, including 10 kb of flanking sequence (NCBI Build 36.1 chromosome 3 position 120,715,830–120,771,171 and chromosome 2 position 204,269,443–204,321,880, respectively) were extracted from the genetic data. Within the 55.3 kb *B7-1* and 52.4 kb *CD28* loci, data for 19 SNPs (12 and 7 SNPs, respectively) were obtained. In addition, genotype data across the *B7-1* locus were augmented by imputation of 57 ungenotyped SNPs across this region using MaCH (www.sph.umich.edu/csg/abecasis/MACH/) software as previously described.³⁷ In total, 69 SNPs (12 genotyped and 57 imputed) with an average intermarker distance of 706 bp were included in our association analysis at the *B7-1* locus.

Deviation from Hardy–Weinberg equilibrium was assessed for use of a genotypic chi-squared test. Genotype data were analyzed using additive tests of association to calculate *P* values and ORs. Quantitative trait analyses were performed using available ACR measurement data and cystatin-based eGFR. All statistical analyses were performed using PLINK.³⁸

Statistical Analyses

Deviation from Hardy–Weinberg equilibrium was assessed for use of a genotypic chi-squared test. Genotype data were analyzed using additive tests of association to calculate *P* values and ORs. Quantitative trait analyses were performed using available ACR measurement data and cystatin-based eGFR. All statistical analyses were performed using PLINK.³⁸

Epidemiologic Studies in the Joslin Clinic Cohort

Cohort of Patients

Epidemiologic studies were performed on the Joslin Clinic cohort of individuals with T2D followed for DN progression. For a more detailed description of patient groups, please refer to Supplemental Table 1. Only patients with increased urinary albumin excretion (UAE) (in the microalbuminuria and proteinuria range) and available plasma samples at baseline were considered eligible for this study. sB7-1 was measured by Instant ELISA (eBioscience, San Diego, CA), whereas sCD28 and sCTLA4 were measured by Platinum ELISA (eBioscience). Assay sensitivities were 0.18 ng/ml for sCD28, 0.10 ng/ml for sB7-1, and 0.13 ng/ml for sCTLA4. In our study, sCD28 was detectable in 90%, sB7-1 in 94%, and sCTLA4 in 4% of plasma samples. ODs of sCD28 and sB7-1 were fitted to a five-parameter logistic standard curve with 1/*y* weighting using Masterplex Readerfit (v.1.1.4.52; Hitachi Software Engineering, Shinagawa, Japan).

Assessment of DN at Baseline

The results of urinalyses performed on these patients' urine during the preceding 2-year interval were reviewed within the Joslin Clinic computer database. The ACR value was converted to an albumin excretion rate (AER) according to a previously published formula.³⁹ For

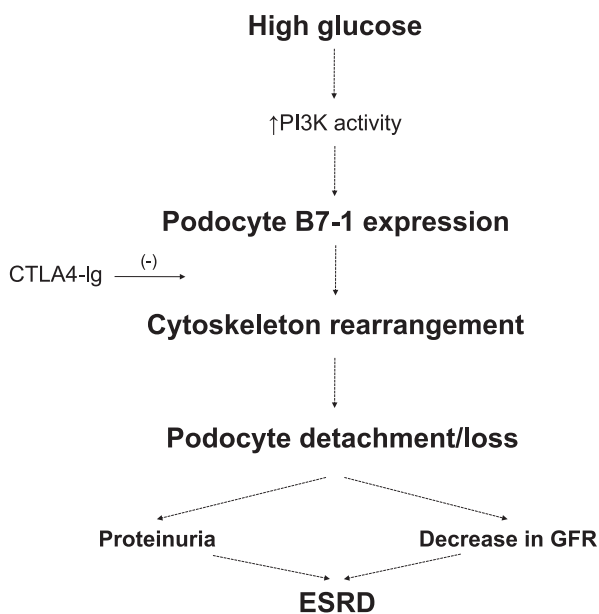


Figure 8. Proposed model to explain the role of B7-1 and CTLA4-Ig action in DN.

each patient, the geometric mean AER for the preceding 2-year interval was determined to assign albuminuria status as follows: microalbuminuria, AER 30–300 mg/min; and macroalbuminuria/proteinuria, >300 mg/min.^{39,40} In 2009, plasma creatinine was measured in stored baseline samples at the University of Minnesota with the Roche enzymatic assay (Roche, Pleasanton, CA) on a Roche/Hitachi Mod P analyzer. GFR was estimated from plasma concentrations of creatinine using the IDMS-traceable Modification of Diet in Renal Disease (MDRD) formula.⁴¹ Individuals with evidence of nephropathy unrelated to diabetes and with CKD stages 4 and 5⁴² were excluded.

Ascertainment of ESRD and Mortality

All individuals were queried against rosters of the US Renal Data System (USRDS) and the National Death Index (NDI) covering all events up to the end of 2004. The USRDS maintains a roster of United States patients receiving RRT and includes dates of dialysis and transplantation.^{43,44} ESRD was defined by a match with the USRDS roster ($n=39$) or a listing of renal failure among the causes of death on an NDI death certificate ($n=16$).

Statistical Analyses

Follow-up data were analyzed as incidence rates of ESRD or death without ESRD and were tested for trend across quartiles of each marker (B7-1 and CD28) distribution. The Cox proportional hazard model was used to evaluate the independent effect of investigated markers. The effect of quartiles of the marker distribution (categorical variable) was examined in the univariate analysis and subsequently with an adjustment by relevant clinical covariates. Statistical analysis was performed with SAS software (version 9.2; SAS Institute, Inc., Cary, NC).

Statistical Analysis

Data are expressed as the mean \pm SEM. When two groups were compared cross-sectionally, two-sided unpaired *t* tests (for parametric data) or Mann–Whitney tests (for nonparametric data) were used according to distribution. ANOVA (for parametric data) and Kruskal–Wallis tests (for nonparametric data) were used. *Post hoc* analysis was chosen to evaluate *a posteriori* pairwise comparisons, and the Bonferroni correction was used to account for multiple comparisons. The chi-squared test for categorical variables was used when necessary. A *P* value <0.05 (by two-tailed testing) was considered an indicator of statistical significance. Data were analyzed using an SPSS statistical package for Windows (SPSS, Inc., Chicago, IL). Prism software was used for drawing graphs (GraphPad Software, Inc., San Diego, CA).

ACKNOWLEDGMENTS

P.F. is the recipient of a Juvenile Diabetes Research Foundation (JDRF) career development award, an American Society of Nephrology career development award, and an American Diabetes Association (ADA) mentor-based fellowship grant. P.F. is also supported by grants from Boston Children's Hospital (Translational Research Program), the Harvard Stem Cell Institute (Diabetes Program DP-0123-12-00), and the Italian Ministry of Health (RF-2010-2303119, RF-2010-2314794,

and RF-FSR-2008-1213704). A.V. is supported by a Associazione Medici Diabetologi (AMD)–Società Italiana di Diabetologia (SID) Pasquale di Coste scholarship, as well as a National Institutes of Health (NIH) research training grant to Boston Children's Hospital in Pediatric Nephrology (T32DK007726-28). A.V. conducted this study as partial fulfillment of his PhD program in Molecular Medicine at San Raffaele University (Milan, Italy). R.B. is supported by an ADA mentor-based fellowship grant to P.F. and by an American Society of Transplantation/Genentech clinical science fellowship grant. R.B. conducted this study as partial fulfillment of his PhD program in Biology and Biotechnology at Salento University (Lecce, Italy). L.B. is supported by the Swedish Research Council and by the Swedish Governmental Agency for Innovation Systems. P.M. is supported by grants from the NIH (DK57683, DK062472, and DK091218). J.R. is supported by grants from the NIH (DK073495, DK089394, DK101350) and A.S.K. is supported by grants from the NIH (DK41526, DK58549 and DK77532).

DISCLOSURES

J.R. has pending or issued patents on novel kidney protective therapies. He stands to receive royalties from their future commercialization.

REFERENCES

1. Olshansky SJ, Passaro DJ, Hershov RC, Layden J, Carnes BA, Brody J, Hayflick L, Butler RN, Allison DB, Ludwig DS: A potential decline in life expectancy in the United States in the 21st century. *N Engl J Med* 352: 1138–1145, 2005
2. Tirosh A, Shai I, Tekes-Manova D, Israeli E, Pereg D, Shochat T, Kochba I, Rudich A; Israeli Diabetes Research Group: Normal fasting plasma glucose levels and type 2 diabetes in young men. *N Engl J Med* 353: 1454–1462, 2005
3. Fiorina P, Folli F, Bertuzzi F, Maffi P, Finzi G, Venturini M, Soccì C, Davalli A, Orsenigo E, Monti L, Falqui L, Uccella S, La Rosa S, Usellini L, Properzi G, Di Carlo V, Del Maschio A, Capella C, Secchi A: Long-term beneficial effect of islet transplantation on diabetic macro-/microangiopathy in type 1 diabetic kidney-transplanted patients. *Diabetes Care* 26: 1129–1136, 2003
4. Nakamura T, Ushiyama C, Suzuki S, Hara M, Shimada N, Ebihara I, Koide H: Urinary excretion of podocytes in patients with diabetic nephropathy. *Nephrol Dial Transplant* 15: 1379–1383, 2000
5. Reiser J, von Gersdorff G, Loos M, Oh J, Asanuma K, Giardino L, Rastaldi MP, Calvaresi N, Watanabe H, Schwarz K, Faul C, Kretzler M, Davidson A, Sugimoto H, Kalluri R, Sharpe AH, Kreidberg JA, Mundel P: Induction of B7-1 in podocytes is associated with nephrotic syndrome. *J Clin Invest* 113: 1390–1397, 2004
6. Festa A, D'Agostino R, Howard G, Mykkanen L, Tracy RP, Haffner SM: Inflammation and microalbuminuria in nondiabetic and type 2 diabetic subjects: The Insulin Resistance Atherosclerosis Study. *Kidney Int* 58: 1703–1710, 2000
7. Menini S, Amadio L, Oddi G, Ricci C, Pesce C, Pugliese F, Giorgio M, Migliaccio E, Pelicci P, Iacobini C, Pugliese G: Deletion of p66Shc longevity gene protects against experimental diabetic glomerulopathy by preventing diabetes-induced oxidative stress. *Diabetes* 55: 1642–1650, 2006
8. Ritz E, Orth SR: Nephropathy in patients with type 2 diabetes mellitus. *N Engl J Med* 341: 1127–1133, 1999
9. Somlo S, Mundel P: Getting a foothold in nephrotic syndrome. *Nat Genet* 24: 333–335, 2000

10. Greenwald RJ, Freeman GJ, Sharpe AH: The B7 family revisited. *Annu Rev Immunol* 23: 515–548, 2005
11. Genovese MC, Becker JC, Schiff M, Luggen M, Sherrer Y, Kremer J, Birbara C, Box J, Natarajan K, Nuamah I, Li T, Aranda R, Hagerty DT, Dougados M: Abatacept for rheumatoid arthritis refractory to tumor necrosis factor alpha inhibition. *N Engl J Med* 353: 1114–1123, 2005
12. Yu CC, Fornoni A, Weins A, Hakrrouch S, Maiguel D, Sageshima J, Chen L, Ciancio G, Faridi MH, Behr D, Campbell KN, Chang JM, Chen HC, Oh J, Faul C, Arnaout MA, Fiorina P, Gupta V, Greka A, Burke GW 3rd, Mundel P: Abatacept in B7-1-positive proteinuric kidney disease. *N Engl J Med* 369: 2416–2423, 2013
13. Tervaert TW, Mooyaart AL, Amann K, Cohen AH, Cook HT, Drachenberg CB, Ferrario F, Fogo AB, Haas M, de Heer E, Joh K, Noël LH, Radhakrishnan J, Seshan SV, Bajema IM, Buijhn JA; Renal Pathology Society: Pathologic classification of diabetic nephropathy. *J Am Soc Nephrol* 21: 556–563, 2010
14. Mundel P, Heid HW, Mundel TM, Krüger M, Reiser J, Kriz W: Synaptopodin: An actin-associated protein in telencephalic dendrites and renal podocytes. *J Cell Biol* 139: 193–204, 1997
15. Mundel P, Reiser J, Zúñiga Mejía Borja A, Pavenstädt H, Davidson GR, Kriz W, Zeller R: Rearrangements of the cytoskeleton and cell contacts induce process formation during differentiation of conditionally immortalized mouse podocyte cell lines. *Exp Cell Res* 236: 248–258, 1997
16. Chuang TD, Guh JY, Chiou SJ, Chen HC, Huang JS, Yang YL, Chuang LY: Phosphoinositide 3-kinase is required for high glucose-induced hypertrophy and p21WAF1 expression in LLC-PK1 cells. *Kidney Int* 71: 867–874, 2007
17. Jain S, De Petris L, Hoshi M, Akilesh S, Chatterjee R, Liapis H: Expression profiles of podocytes exposed to high glucose reveal new insights into early diabetic glomerulopathy. *Lab Invest* 91: 488–498, 2011
18. Schaller MD: Paxillin: A focal adhesion-associated adaptor protein. *Oncogene* 20: 6459–6472, 2001
19. Dai C, Stolz DB, Bastacky SI, St-Arnaud R, Wu C, Dedhar S, Liu Y: Essential role of integrin-linked kinase in podocyte biology: bridging the integrin and slit diaphragm signaling. *J Am Soc Nephrol* 17: 2164–2175, 2006
20. Brosius FC 3rd, Alpers CE, Bottinger EP, Breyer MD, Coffman TM, Gurley SB, Harris RC, Kakoki M, Kretzler M, Leiter EH, Levi M, McIndoe RA, Sharma K, Smithies O, Susztak K, Takahashi N, Takahashi T; Animal Models of Diabetic Complications Consortium: Mouse models of diabetic nephropathy. *J Am Soc Nephrol* 20: 2503–2512, 2009
21. Chandraker A, Azuma H, Nadeau K, Carpenter CB, Tilney NL, Hancock WW, Sayegh MH: Late blockade of T cell costimulation interrupts progression of experimental chronic allograft rejection. *J Clin Invest* 101: 2309–2318, 1998
22. Maffi P, Bertuzzi F, De Taddeo F, Magistretti P, Nano R, Fiorina P, Caumo A, Pozzi P, Soggi C, Venturini M, del Maschio A, Secchi A: Kidney function after islet transplant alone in type 1 diabetes: Impact of immunosuppressive therapy on progression of diabetic nephropathy. *Diabetes Care* 30: 1150–1155, 2007
23. Krolewski AS, Warram JH, Freire MB: Epidemiology of late diabetic complications. A basis for the development and evaluation of preventive programs. *Endocrinol Metab Clin North Am* 25: 217–242, 1996
24. Rosolowsky ET, Skupien J, Smiles AM, Niewczas M, Roshan B, Stanton R, Eckfeldt JH, Warram JH, Krolewski AS: Risk for ESRD in type 1 diabetes remains high despite renoprotection. *J Am Soc Nephrol* 22: 545–553, 2011
25. Bolton WK, Cattran DC, Williams ME, Adler SG, Appel GB, Cartwright K, Foiles PG, Freedman BI, Raskin P, Ratner RE, Spinowitz BS, Whittier FC, Wuerth JP; ACTION I Investigator Group: Randomized trial of an inhibitor of formation of advanced glycation end products in diabetic nephropathy. *Am J Nephrol* 24: 32–40, 2004
26. Mauer M, Zinman B, Gardiner R, Suissa S, Sinaiko A, Strand T, Drummond K, Donnelly S, Goodyer P, Gubler MC, Klein R: Renal and retinal effects of enalapril and losartan in type 1 diabetes. *N Engl J Med* 361: 40–51, 2009
27. Patel A, MacMahon S, Chalmers J, Neal B, Woodward M, Billot L, Harrap S, Poulter N, Marre M, Cooper M, Glasziou P, Grobbee DE, Hamet P, Heller S, Liu LS, Mancia G, Mogensen CE, Pan CY, Rodgers A, Williams B; ADVANCE Collaborative Group: Effects of a fixed combination of perindopril and indapamide on macrovascular and microvascular outcomes in patients with type 2 diabetes mellitus (the ADVANCE trial): A randomised controlled trial. *Lancet* 370: 829–840, 2007
28. Shan D, Wu HM, Yuan QY, Li J, Zhou RL, Liu GJ: Pentoxifylline for diabetic kidney disease. *Cochrane Database Syst Rev* 2: CD006800, 2012
29. Doria A, Niewczas MA, Fiorina P: Can existing drugs approved for other indications retard renal function decline in patients with type 1 diabetes and nephropathy? *Semin Nephrol* 32: 437–444, 2012
30. Pergola PE, Raskin P, Toto RD, Meyer CJ, Huff JW, Grossman EB, Krauth M, Ruiz S, Audhya P, Christ-Schmidt H, Wittes J, Warnock DG; BEAM Study Investigators: Bardoxolone methyl and kidney function in CKD with type 2 diabetes. *N Engl J Med* 365: 327–336, 2011
31. Kremer JM, Westhovens R, Leon M, Di Giorgio E, Alten R, Steinfeld S, Russell A, Dougados M, Emery P, Nuamah IF, Williams GR, Becker JC, Hagerty DT, Moreland LW: Treatment of rheumatoid arthritis by selective inhibition of T-cell activation with fusion protein CTLA4Ig. *N Engl J Med* 349: 1907–1915, 2003
32. Ruperto N, Lovell DJ, Quartier P, Paz E, Rubio-Pérez N, Silva CA, Abud-Mendoza C, Burgos-Vargas R, Gerloni V, Melo-Gomes JA, Saad-Magalhães C, Sztajn bok F, Goldenstein-Schainberg C, Scheinberg M, Penades IC, Fischbach M, Orozco J, Hashkes PJ, Hom C, Jung L, Lepore L, Oliveira S, Wallace CA, Sigal LH, Block AJ, Covucci A, Martini A, Giannini EH; Paediatric Rheumatology International Trials Organization/Pediatric Rheumatology Collaborative Study Group: Abatacept in children with juvenile idiopathic arthritis: A randomised, double-blind, placebo-controlled withdrawal trial. *Lancet* 372: 383–391, 2008
33. E Astorri, P Fiorina, G Gavaruzzi, A Astorri, G Magnati: Left ventricular function in insulin-dependent and in non-insulin-dependent diabetic patients: radionuclide assessment. *Cardiology* 88: 152–155, 1997
34. Eid AA, Ford BM, Bhandary B, de Cassia Cavaglieri R, Block K, Barnes JL, Gorin Y, Choudhury GG, Abboud HE: Mammalian target of rapamycin regulates Nox4-mediated podocyte depletion in diabetic renal injury. *Diabetes* 62: 2935–2947, 2013
35. Fischer R, Julsgart J, Berchtold MW: High affinity calmodulin target sequence in the signalling molecule PI 3-kinase. *FEBS Lett* 425: 175–177, 1998
36. Pezzolesi MG, Poznik GD, Skupien J, Smiles AM, Mychaleckyj JC, Rich SS, Warram JH, Krolewski AS: An intergenic region on chromosome 13q33.3 is associated with the susceptibility to kidney disease in type 1 and 2 diabetes. *Kidney Int* 80: 105–111, 2011
37. Pezzolesi MG, Poznik GD, Mychaleckyj JC, Paterson AD, Barati MT, Klein JB, Ng DP, Placha G, Canani LH, Bochenski J, Waggott D, Merchant ML, Krolewski B, Mirea L, Wanik K, Katavetin P, Kure M, Wolkow P, Dunn JS, Smiles A, Walker WH, Boright AP, Bull SB, Doria A, Rogus JJ, Rich SS, Warram JH, Krolewski AS; DCCT/EDIC Research Group: Genome-wide association scan for diabetic nephropathy susceptibility genes in type 1 diabetes. *Diabetes* 58: 1403–1410, 2009
38. Purcell S, Neale B, Todd-Brown K, Thomas L, Ferreira MA, Bender D, Maller J, Sklar P, de Bakker PI, Daly MJ, Sham PC: PLINK: A tool set for whole-genome association and population-based linkage analyses. *Am J Hum Genet* 81: 559–575, 2007
39. Krolewski AS, Laffel LM, Krolewski M, Quinn M, Warram JH: Glycosylated hemoglobin and the risk of microalbuminuria in patients with insulin-dependent diabetes mellitus. *N Engl J Med* 332: 1251–1255, 1995
40. Niewczas MA, Gohda T, Skupien J, Smiles AM, Walker WH, Rosetti F, Cullere X, Eckfeldt JH, Doria A, Mayadas TN, Warram JH, Krolewski AS: Circulating TNF receptors 1 and 2 predict ESRD in type 2 diabetes. *J Am Soc Nephrol* 23: 507–515, 2012

41. Levey AS, Coresh J, Greene T, Marsh J, Stevens LA, Kusek JW, Van Lente F; Chronic Kidney Disease Epidemiology Collaboration: Expressing the Modification of Diet in Renal Disease Study equation for estimating glomerular filtration rate with standardized serum creatinine values. *Clin Chem* 53: 766–772, 2007
42. Folli F, Guzzi V, Perego L, Coletta DK, Finzi G, Placidi C, La Rosa S, Capella C, Socci C, Lauro D, Tripathy D, Jenkinson C, Paroni R, Orsenigo E, Cighetti G, Gregorini L, Staudacher C, Secchi A, Bachi A, Brownlee M, Fiorina P: Proteomics reveals novel oxidative and glycolytic mechanisms in type 1 diabetic patients' skin which are normalized by kidney-pancreas transplantation. *PLoS ONE* 5: e9923, 2010
43. Agodoa LY, Eggers PW: Renal replacement therapy in the United States: Data from the United States Renal Data System. *Am J Kidney Dis* 25: 119–133, 1995
44. Cowper DC, Kubal JD, Maynard C, Hynes DM: A primer and comparative review of major US mortality databases. *Ann Epidemiol* 12: 462–468, 2002

This article contains supplemental material online at <http://jasn.asnjournals.org/lookup/suppl/doi:10.1681/ASN.2013050518/-/DCSupplemental>.